Surface states and Fermi-level pinning at epitaxial Pb/Si(111) surfaces

H. H. Weitering,* A. R. H. F. Ettema, and T. Hibma
Laboratory of Inorganic Chemistry, Materials Science Centre, University of Groningen, Nijenborgh 16, 9747 AG Groningen, The Netherlands
(Received 6 March 1991; revised manuscript received 4 October 1991)

The difference in Schottky-barrier height of epitaxial Si(111) $(\sqrt{3}\times\sqrt{3})R30°$-Pb($\beta$) and Si(111)(7×7)-Pb interfaces, supports the view that the Schottky-barrier height at these interfaces is not determined by bulk properties of the metal and the semiconductor, but that it depends on the local geometry and electronic structure at the interface. To elucidate the relation between the interface electronic structure and the Schottky-barrier height, we performed an angle-resolved photoemission study on the Si(111)(7×7)-Pb and the Si(111)$(\sqrt{3}\times\sqrt{3})R30°$-Pb($\beta$) surfaces. The electronic structures of these two surfaces are rather similar. Two different surface-state bands were resolved. One of them is fully occupied and is situated below the valence-band maximum (VBM). This state is interpreted as a Si dangling-bond state that is hybridized with Pb $6p_x,p_y$ orbitals. The other state pins the Fermi level at approximately 0.1 eV above the VBM. This state has no measurable dispersion and appears in regions of **k** space where a common gap is present in the projected band structure of Pb and Si. Therefore, this surface state may become a true interface state at thick overlayers, pinning the Fermi level of the Si(111)$(\sqrt{3}\times\sqrt{3})R30°$-Pb($\beta$) Schottky diodes near the bottom of the energy gap.

I. INTRODUCTION

Recently we reported a remarkable difference in the Schottky-barrier height (SBH) of two different epitaxially grown Pb/Si(111) contacts.[1] Diodes, having a Si(111)(7×7)-Pb interface, have an *n*-type SBH of 0.70 eV while diodes with the Si(111)$(\sqrt{3}\times\sqrt{3})R30°$-Pb($\beta$) interface have a SBH of 0.93 eV. These SBH were measured with capacitance-voltage (*C-V*) and current-voltage (*I-V*) techniques. This difference cannot be explained on the basis of the bulk properties of Pb and Si, and so it must be caused by differences in the local electronic structure at the interface. A similar atomic-structure dependence of the SBH has been observed previously at epitaxial $NiSi_2$/Si contacts.[2]

The Fermi-level position at the 7×7 interface is close to the charge neutrality level (CNL) of Tersoff's metal-induced-gap-state (MIGS) theory.[3] However, the barrier height at the $\sqrt{3}\times\sqrt{3}$ interface is extremely high. This requires a high density of interface states near the bottom of the energy gap, at or below 0.93 eV below the conduction-band edge.[1,4] The Fermi-level position at this interface is fully determined by the spectral distribution of the interface states and is almost independent of the work function of the metal. This phenomenon is called Fermi-level pinning.[5] In order to understand the observed SBH's, we have to identify these interface states. This is not an easy task, because it is hardly possible to probe the electronic states at a deeply buried interface. However, at metal coverages of one or a few monolayers, photoelectron spectroscopy can be used to probe the electronic structure in a direct way. Also the Fermi-level position at monolayer coverage can be deduced from photoemission experiments.

From core-level photoemission studies, Le Lay and coworkers[6] already derived *n*-type SBH's of approximately 0.9 and 1.0 eV for the Si(111)(7×7)-Pb and Si(111)$(\sqrt{3}\times\sqrt{3})R30°$-Pb($\beta$) surfaces, respectively. These measurements were performed on both *n*- and *p*-type samples at monolayer coverage. The discrepancy between the SBH's of the Si(111)(7×7)-Pb contacts at monolayer coverage and at fully established (7×7) interfaces has been a matter of debate.[7] However, the Schottky barriers of the $\sqrt{3}\times\sqrt{3}$ diodes are rather close to those at monolayer coverage.

In order to understand the relation between the interface structures and the SBH, we studied the evolution of the structural and electronic properties in the early stages of interface formation for the Si(111)(7×7)-Pb and Si(111)$(\sqrt{3}\times\sqrt{3})R30°$-Pb($\beta$) systems. In this paper we will give a detailed account of our angle-resolved ultraviolet photoelectron spectroscopy study (ARUPS). In a separate paper, we report on the structural properties of these interfaces.[8] It will be shown that at a coverage of one monolayer of Pb two new surface states have shown up, and that the Fermi level is pinned near the valence-band maximum (VBM). This means that the *n*-type SBH's of these monolayer phases are extremely high. We will discuss the relation between the SBH's inferred at monolayer coverage and those at thick diodes.

The Ge(111)$\sqrt{3}\times\sqrt{3})R30°$-Pb($\beta$) surface has already been studied with ARUPS by Tonner *et al.*[9] The structure of this surface has already been determined with grazing incidence x-ray diffraction,[10] x-ray standing wave experiments,[11] and low-energy electron diffraction (LEED) *I-V* analysis.[12] This so-called β phase essentially consists of a close-packed hexagonal Pb layer which is rotated 30° with respect to the hexagonal Ge(111) lattice. The saturation coverage is $\frac{4}{3}$ monolayers (ML) in substrate units. This surface is closely related to the Si(111)

$(\sqrt{3}\times\sqrt{3})R30°$-Pb($\beta$) surface. However, a small difference is that the two-dimensional Pb layer is perfectly commensurate with the Ge(111) lattice while it is slightly compressed and incommensurate on Si(111).[8] This is due to the slightly smaller lattice parameter of Si. We will show that the electronic structures of these $\sqrt{3}\times\sqrt{3}$ phases on Si(111) and Ge(111) are rather similar. However, a remarkable difference is that the Ge(111) $(\sqrt{3}\times\sqrt{3})R30°$-Pb($\beta$) surface is semiconducting[9] while the related Pb/Si(111) surfaces are metallic.[6,13]

II. EXPERIMENT

The photoemission experiments were performed in an ADES 400 spectrometer equipped with a He discharge lamp, an x-ray source for both Al $K\alpha$ (1486.6 eV) and Mg $K\alpha$ (1253.6 eV) radiation, a conventional LEED apparatus, and an angle-resolving hemispherical electron energy analyzer. The angle resolution of the analyzer is 2°. The energy resolution is approximately 0.1 eV. The system is also equipped with a Pb evaporation source. The evaporation rate was calibrated by determining the kink in the intensity versus coverage plot for the Pb $4f_{7/2}$ XPS core-level signal. We used an evaporation rate of 1 ML per 150 sec. The pressure during the evaporation was below 10^{-9} mbar.

We also performed ARUPS experiments using polarized radiation produced by the synchrotron at the SERC Daresbury Laboratory (United Kingdom). These spectra were recorded with only a moderate angle resolution (3.5°). The energy resolution of the spectra is approximately 0.2 eV. This ADES 400 spectrometer is also equipped with a retarding field Auger spectrometer, which was used for calibrating the evaporation rate (1 ML per 180 sec).

Details about the sample treatment are found in Ref. 1. We used n-type Si(111) wafers having a resistivity of 8.6 Ω cm ($N_D \approx 2\times10^{14}/\text{cm}^3$). The presence of the three well-known surface states in the UPS spectrum was considered as a quality check for the clean Si(111)(7×7) surface.

III. ANGLE-RESOLVED ULTRAVIOLET PHOTOELECTRON SPECTRA (UPS)

Angle-resolved UPS spectra of the clean reconstructed Si(111)(7×7) surface, the Si(111)(7×7)-Pb surface, and the Si(111)$(\sqrt{3}\times\sqrt{3})R30°$-Pb($\beta$) surface were recorded. The initial energies and parallel wave vectors were calculated from the following relations[14]:

$$E_{\text{kin}} = \hbar\omega - E_i - \Phi_s \ , \tag{1}$$

$$\hbar|\mathbf{k}_\parallel| = \sin\theta\sqrt{2mE_{\text{kin}}} \ . \tag{2}$$

The initial energy E_i is defined with respect to the Fermi level. The angle θ is defined as the detector angle with respect to the surface normal. The sample work function Φ_s was determined by measuring the secondary cutoff in the UPS spectrum at a different sample bias. The parallel wave vector $\mathbf{k}_\parallel$ was along the $[1\bar{1}0]$ and $[2\bar{1}\bar{1}]$ azimuths of the Si lattice which corresponds to the $\bar{\Gamma}\bar{K}$ and $\bar{\Gamma}\bar{M}$ directions in the 1×1 surface Brillouin zone (SBZ) (Fig. 1). In the next two sections, we will discuss the coverage dependence and angle dependence of the photoemission spectra.

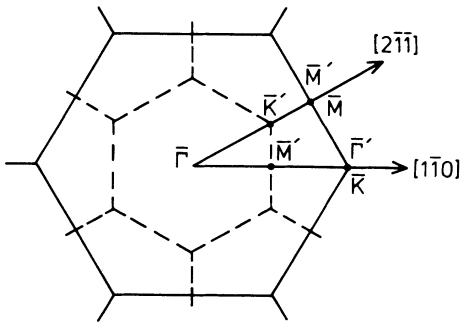

FIG. 1. The 1×1 and $\sqrt{3}\times\sqrt{3}$ surface Brillouin zones of the Si(111) surface (solid and dashed lines, respectively).

A. Coverage-dependent UPS

In Figs. 2 and 3 we show the evolution of the UPS spectra with the deposition of Pb, using unpolarized He I (21.2-eV) radiation, at fixed emission angles of 22.5° and 0°, respectively.

The lowest spectrum in Figs. 2 and 3 belongs to the clean Si(111)(7×7) surface. The well-known S_1, S_2, and

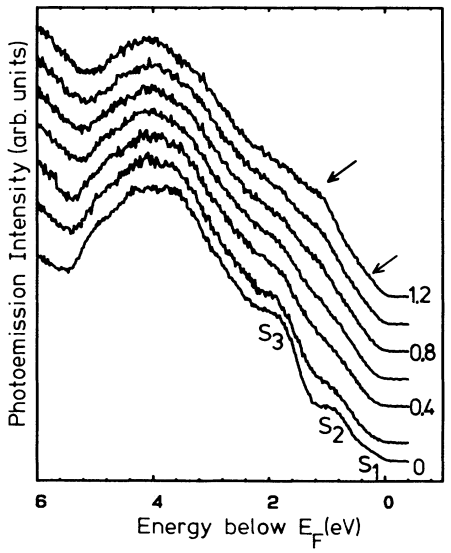

FIG. 2. Angle-resolved UPS spectra (incident angle $\alpha_i = 45°$, $\theta = 22.5°$) of the Si(111)(7×7) surface with different overlayers of Pb, deposited at room temperature. The coverages are indicated by the numbers at the right side of each spectrum. The lowest spectrum corresponds to the clean Si(111)(7×7) surface. The surface states S_1, S_2, and S_3 are indicated. The uppermost spectrum corresponds to the Si(111)(7×7)-Pb surface. The shoulders, indicated by arrows, are the Pb-induced surface states. The spectra are recorded along the $\bar{\Gamma}\bar{K}$ direction, using unpolarized He I radiation (21.2 eV).

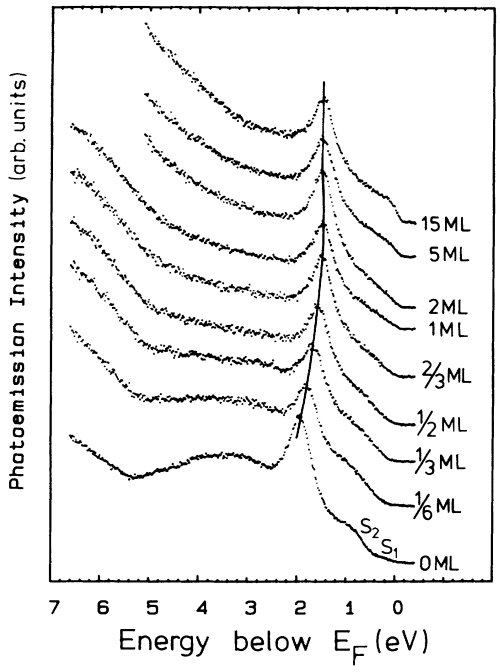

FIG. 3. Angle-resolved UPS spectra ($\alpha_1=17.5°$, $\theta=0°$) of the Si(111)(7×7) surface with different overlayers of Pb, deposited at room temperature. The coverages are indicated by the numbers at the right side of each spectrum. The lowest spectrum corresponds to the clean Si(111)(7×7) surface. The surface states S_1 and S_2 are indicated. The sharp peak is attributed to a direct transition from the uppermost valence band of Si to a free-electron-like final state (Ref. 20). The solid line follows the shift of this bulk-state emission toward E_F as the coverage increases. This shift is due to band bending. The spectra are recorded with unpolarized He I radiation (21.2 eV).

S_3 surface states of the Si(111)(7×7) surface are indicated. The deep-lying S_3 surface state is the so-called backbond surface state and is composed of Si dangling bond states. These states are hybridized with the p_x and p_y orbitals of the adatoms which are present at the 7×7 reconstructed surface. The S_2 and S_1 surface states are localized at the restatoms and adatoms, respectively. For a more detailed discussion of the ARUPS spectra of the Si(111)(7×7) surface, we refer to Hansson and Uhrberg.[15]

At an emission angle of 22.5° all Si(111) surface states are visible. From Fig. 2 it is clear that the S_1 and S_2 surface states rapidly disappear long before the first monolayer is completed (approximately 1.3 Pb atom per Si surface atom). The S_3 state seems to survive a bit longer. At a coverage of 1 ML, two new Pb-induced surface states have shown up. One of them is close to the Fermi level while the other appears as a broad shoulder and is situated approximately 0.9 eV below the Fermi level. These states are situated in the gap of the projected band structure of Si and are therefore real surface states, as will be discussed in Sec. V. These states do not emerge in the spectra as sharp peaks as might be expected for surface-state emission. Several mechanisms may be responsible for the broadening of the surface-state features. First, a random occupancy disorder is present. Second, the surface exhibits a 7×7 periodicity and the photoelectrons will suffer strong Umklapp scattering at this surface. And finally, the features from the UPS spectra will be composed of unresolved sets of surface-state bands, because there are a lot of symmetry inequivalent Pb sites in a 7×7 unit cell.

At normal emission, the S_1 and S_2 surface states are visible together with a prominent bulk feature at 1.8 eV below E_F (Fig. 3). This features does not correspond to the S_3 surface state as pointed out by Hansson and Uhrberg.[15] The latter state only becomes visible at emission angles larger than 15° (He I). From this figure, it is evident that on depositing Pb, this bulk feature shifts toward the Fermi level. This rigid shift is linear with the coverage and stops abruptly at a coverage of 0.8 ML. The magnitude of this shift is very close to the rigid shift in the high-resolution Si $2p$ core-level spectra of Hricovini and Le Lay.[16,6] Therefore it is very likely that this shift is solely due to band bending and that possible hybridization effects are negligible. From the rigid shift of the valence bands in the UPS spectra, we calculate the SBH. The evolution of the n-type SBH is displayed in Fig. 4, together with the photoemission intensity of the Pb $4f_{7/2}$ core level. The kink in the latter data marks the point where the first monolayer is completed. The final shift in the UPS spectra is 0.45±0.05 eV. Because the Fermi level of the clean 7×7 surface is pinned 0.63±0.05 eV above the valence-band edge,[17] the final position of the Fermi level will be 0.18±0.10 eV above the valence-band edge, leading to an n-type SBH of 0.94±0.10 eV.

After annealing the Si(111)(7×7)-Pb phase at 300 °C, we obtain the Si(111)$\sqrt{3}\times\sqrt{3}$)R30°-Pb(β) phase and the valence bands undergo an additional shift of 0.10±0.05 eV toward the Fermi level. A similar shift has been re-

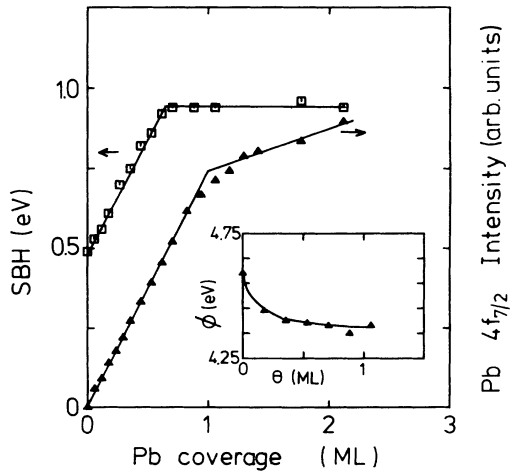

FIG. 4. The Schottky-barrier height, calculated from the shift in binding energy using the data shown in Fig. 3, increases linearly with the coverage. A comparison with the intensity of the $4f_{7/2}$ XPS line shows that band bending stops abruptly before a monolayer is completed. Inset: work function change determined from the width of the UPS spectrum at normal emission.

ported by Hricovini and Le Lay, using high-resolution Si $2p$ core-level spectroscopy.[16,6] Therefore the SBH of the Si(111)($\sqrt{3}\times\sqrt{3}$)R30°-Pb(β) phase at monolayer coverage is 1.04±0.10 eV. Because the band gap of Si is 1.12 eV, this means that the pinning at this incommensurate phase occurs very close to the valence-band edge.

So far, we neglected the surface photovoltage effect.[18] During the photoemission experiment, the excitation of charge carriers across the band gap leads to the generation of a surface photovoltage. This photovoltage tends to suppress the band bending so it is expected that the high Schottky barriers as determined with photoemission may even be too low. Especially for such high barriers ($\approx$1 eV) on lightly doped samples ($N_D \approx 2\times10^{14}/\text{cm}^3$), the possibility of a photovoltage-induced shift of the photoelectron spectra must be explored. Bauer *et al.* used a simple model, based on the recombination of charge carriers by thermionic emission and tunneling, to calculate the surface photovoltage effect as a function of dopant concentration and temperature for p-type GaAs(110).[18] This model can also be applied to calculate the photovoltage effect for our lightly doped Si(111) samples at room temperature. Neglecting tunnel currents, we verified that the photovoltage-induced shift of our UPS spectra should indeed be negligible. Moreover, we also have experimental evidence that the photovoltage effect can be neglected. First of all, we do not observe a shift of the Fermi-level emission relative to that of the external reference level (sample holder). Second, we do not observe a shift of the Fermi edge as we deposit thick metallic overlayers. Finally, the Fermi-level positions at monolayer coverage are reported to be identical for n- and p-type samples.[6] Because the photovoltage effect would induce an opposite shift for n- and p-type samples, we conclude that the photovoltage-induced shift in our spectra is negligible.

The linear increase of the SBH usually suggests that the submonolayer regime is a two-phase system. One is the clean 7×7 surface with a pinning level 0.63 eV above the valence-band maximum and the other is the Si(111)(7×7)-Pb structure with its pinning level 0.18 eV above the valence-band maximum. However the presence of such a two-phase system should be apparent from a broadening or a splitting of the core-level spectra as is nicely illustrated for the Si(111)($\sqrt{3}\times\sqrt{3}$)R30°-Ag surface.[19] Our core-level spectra only show a rigid shift and broadening is not observed.[20] This is in agreement with the core-level spectra of Hricovini and Le Lay.[16,6] Therefore we must reject this explanation. Because little is known about the evolution of the Si(111)(7×7)-Pb structure in the submonolayer range, other explanations will remain highly speculative.

The strong emission at the Fermi level at coverages far beyond 1 ML is due to emission from three-dimensional metallic Pb islands. This Fermi edge was also used as an additional check for the calibration of the spectrometer work function.

We also measured the sample work function change during deposition. This change is shown in the inset of Fig. 4. Its decrease with coverage cannot be explained by the extra negative charging of the surface, which is due to the Fermi-level pinning near the bottom of the energy gap. For this moderately doped sample showing a final band bending shift of 1 eV, the estimated surface charge density balancing the positive charge in the depletion region is only about $1.5\times10^{-4}e^-$ per surface atom. Therefore it is more likely that the work function decrease is due to an additional surface dipole created by the covalent bonding of the Pb atoms to the substrate atoms. A similar decrease was also observed for Al, Ga, and In on Si(111) by Margaritondo, Rowe, and Christman.[21] From the initial slope of the work function versus coverage plot,[22] they estimated the dipole charges per surface atom. Applying the same method for Pb on Si(111) yields a lower limit for the dipole charge of $0.05e^-$ per surface atom. Note that the lowering of the total surface dipole reflects the electronegativity differences between substrate atoms and adsorbate atoms.

B. Angle-resolved UPS

In Fig. 5 we show the angle-dependent UPS spectra of the Si(111)(7×7)-Pb surface along the $\bar{\Gamma}\bar{K}$ direction of the 1×1 SBZ. These spectra were taken using polarized light with photon energies of 21.2 and 40.8 eV, respectively. The spectra measured at a photon energy of 21.2 eV show a pronounced peak above the Fermi level. This emission is an artifact, because it originates from the Pb $5d$ core levels which are ionized by second-order radiation coming from the monochromator. The bulk emissions of the Si substrate have already been extensively studied.[23] Apart from the band bending shifts, there are only minor changes in the valence bands. Therefore we will focus on the surface-state features. In Figs. 6 and 7 the angle-dependent spectra of the Si(111)($\sqrt{3}\times\sqrt{3}$)R30°-Pb(β) surface are shown. These spectra were taken with polarized radiation of 21.2, 31, and 40.8 eV,

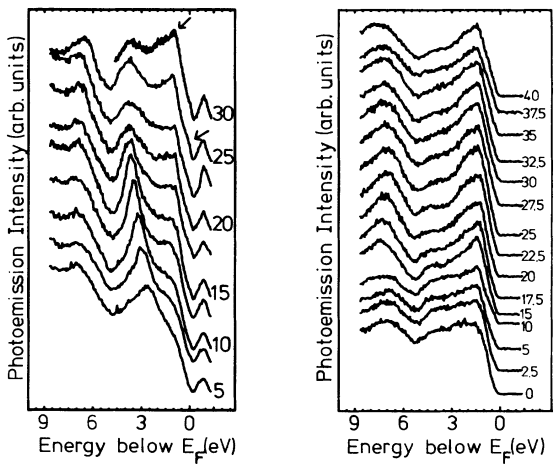

FIG. 5. ARUPS spectra of the Si(111)(7×7)-Pb surface along $\bar{\Gamma}\bar{K}$. The light source is polarized synchrotron radiation with photon energies of 21.2 eV (left) and 40.8 eV (right). The satellite above the Fermi level at 21.2 eV is due to Pb $5d$ photoelectrons, excited by second-order radiation. Surface states are indicated by arrows (left). The incident angle is 45° and the polarization vector is in the emission plane. The numbers indicate the emission angle θ of the photoelectrons.

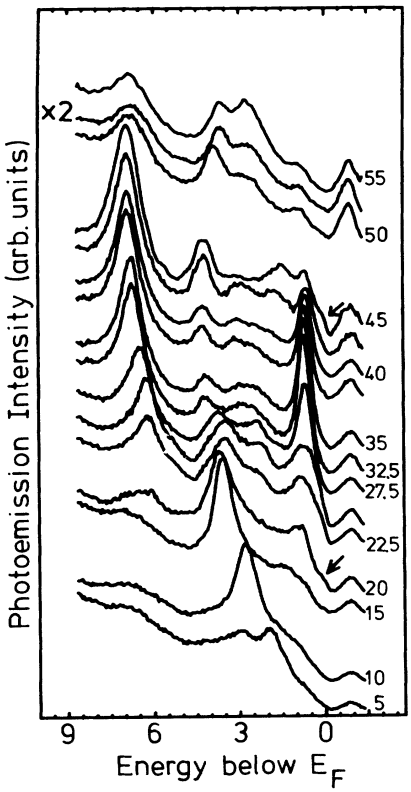

FIG. 6. ARUPS spectra of the Si(111)($\sqrt{3}\times\sqrt{3}$)R30°-Pb(β) surface along $\bar{\Gamma}\bar{K}$. Polarized synchrotron radiation of 21.2 eV is used. The satellite above E_F is due to second-order radiation. The pinning state is indicated by the arrow. The excitation conditions are similar to those of Fig.5. The numbers at the right are the emission angles of the photoelectrons.

respectively. We also recorded ARUPS spectra along the $\bar{\Gamma}\bar{M}$ direction using unpolarized He I radiation. These spectra are not shown but the data of all spectra are summarized in Figs. 8–10 as dispersion plots. For both types of surfaces, two surface-state bands can be distinguished. These bands are situated in the gap of the projected bands structure as will be discussed in Sec. V. The surface state near the Fermi level is poorly resolved, so it is difficult to determine its dispersion. However, it is quite clear that this state is present at E_F in most regions of k space. Because this surface state can easily be detected with UPS, its areal density must be sufficiently high to pin the Fermi level at the surface.[24] For the Si(111)(7×7)-Pb surface, the second surface-state band is located at 0.9 eV below E_F. A similar surface-state band appears as a very strong and sharply peaked surface state in the ARUPS spectra of the incommensurate phase. It is located at approximately 0.8 eV below E_F and has a bandwidth of about 0.4 eV. Because the surface-state dispersions of both structures are rather similar, we will focus our attention on the electronic structure of the $\sqrt{3}\times\sqrt{3}$ phase.

The spectra of the Si(111)($\sqrt{3}\times\sqrt{3}$)R30°-Pb(β) surface are remarkably similar to those of the Ge(111)($\sqrt{3}\times\sqrt{3}$)R30°-Pb(β) surface, which were reported by Tonner *et al.*[9] However, an important difference is that the Si(111)($\sqrt{3}\times\sqrt{3}$)R30°-Pb(β) surface shows emission at the Fermi level while the Ge(111)($\sqrt{3}\times\sqrt{3}$)R30°-Pb(β) surface is semiconducting. The lowest-lying surface-state band at the Si(111)($\sqrt{3}\times\sqrt{3}$)R30°-Pb(β) and Ge(111)($\sqrt{3}\times\sqrt{3}$)R30°-Pb(β) surfaces becomes apparent for $|\mathbf{k}_\parallel| > 0.5$

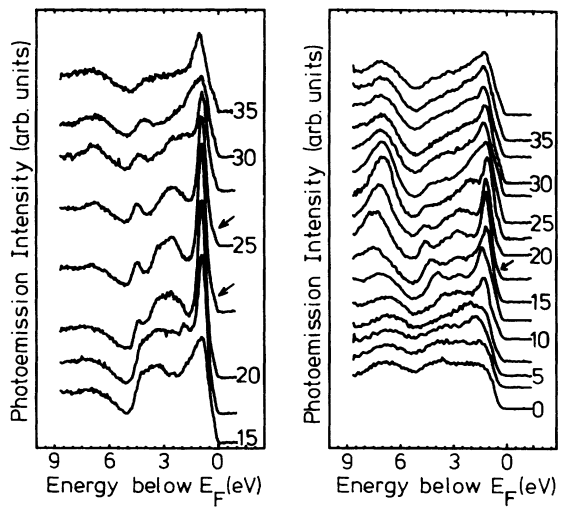

FIG. 7. ARUPS spectra of the Si(111)($\sqrt{3}\times\sqrt{3}$)R30°-Pb(β) surface along $\bar{\Gamma}\bar{K}$. Polarized synchrotron radiation of 31 eV (left) and 40.8 eV (right) is used. Pinning states are indicated by arrows. The excitation conditions are similar to those of Fig. 5. The numbers indicate the emission angle θ of the photoelectrons.

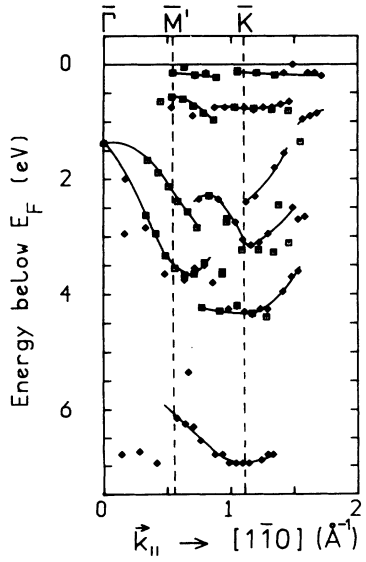

FIG. 8. Experimental dispersion of the Si(111)($\sqrt{3}\times\sqrt{3}$)R30°-Pb(β) surface. The dispersion is calculated by the use of Eqs. (1) and (2). Filled symbols are data from polarized radiation of 2.12 eV (angle resolution 3.5°). Open squares are data obtained with unpolarized He I radiation (21.2 eV). Solid lines are a guide to the eye.

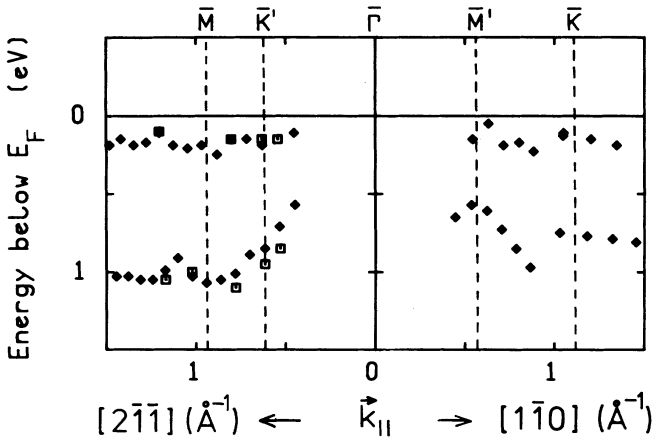

FIG. 9. Detailed surface-state dispersion along the $\bar{\Gamma}\bar{M}$ and $\bar{\Gamma}\bar{K}$ directions of the Si(111)($\sqrt{3}\times\sqrt{3}$)R30°-Pb(β) surface. Data are obtained with unpolarized He I radiation (angle resolution 2°). Open squares are data obtained with an incident angle of 17.5°. The other symbols are data obtained with an incident angle of 45°.

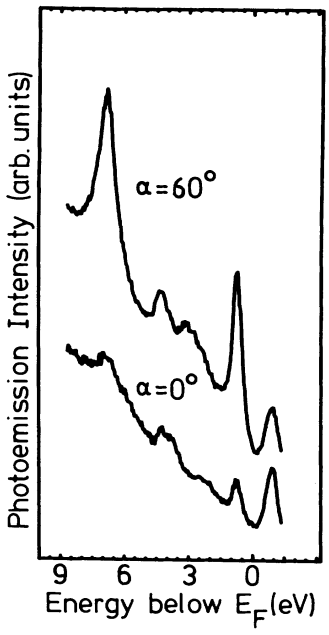

FIG. 11. Incident-angle dependence of the surface-state emission at the Si(111)($\sqrt{3}\times\sqrt{3}$)R30°-Pb(β) surface. The spectra are obtained along $\bar{\Gamma}\bar{K}$ ($\theta=30°$) using polarized synchrotron radiation (21.2 eV). The polarization vector lies in the plane containing the surface normal and the [1$\bar{1}$0] azimuth. The spectra are scaled on the second-order radiation satellite above E_F.

Å and disperses downwards for increasing $\mathbf{k}_{\parallel}$ reaching its minimum near the edges of the 1×1 surface Brillouin zone.

Valuable information about the character of the surface-state wave functions can be obtained by recording the UPS spectra under various excitation conditions. For convenience, we define the surface plane as the x,y plane. The z axis is chosen along the surface normal. The dependence of the emission intensity on the angle of light incidence reveals to what extent the initial-state wave function has z character. Also, the initial-state symmetry can be determined by a proper choice of the direction of the polarization vector **A**. In Fig. 11 we show the incident angle dependence of the surface-state emission at 0.8 eV below E_F. The polarization vector of the radiation is parallel to the plane containing the surface normal and the [1$\bar{1}$0] azimuth (i.e., the emission plane). The emission intensity is strongly reduced at normal incidence. Therefore, this state has considerable z character and must have even symmetry with respect to the emission plane. We conclude that this surface state must be mainly composed of p_z or dangling-bond-type orbitals. Tonner *et al.*[9] observed a similar behavior for the related surface-state emission at the Ge(111)($\sqrt{3}\times\sqrt{3}$)R30°-Pb(β) surface. In addition, they measured this surface-state emission with the polarization vector perpendicular to the emission plane. They showed that in this even-state forbidden geometry, still some emission is left. This must be due to some admixture of p_x and p_y orbitals. Because of the similarity between the surface-state emission of both surfaces, it is therefore likely that for both systems, the lowest-lying surface state has strong z character (or dangling-bond character) while some x,y character is mixed in.

The situation for the pinning state is less clear. No significant polarization or angular dependence could be observed. Because this state cannot be properly resolved, definite conclusions about its orbital symmetry cannot be drawn. This state bears a strong resemblance with the pinning state at the clean 7×7 reconstructed surface. A similar state was also observed by Tonner *et al.*[9] for the Ge(111)($\sqrt{3}\times\sqrt{3}$)R30°-Pb(β) surface, although in that case it is situated 0.45 eV below the valence-band maximum.

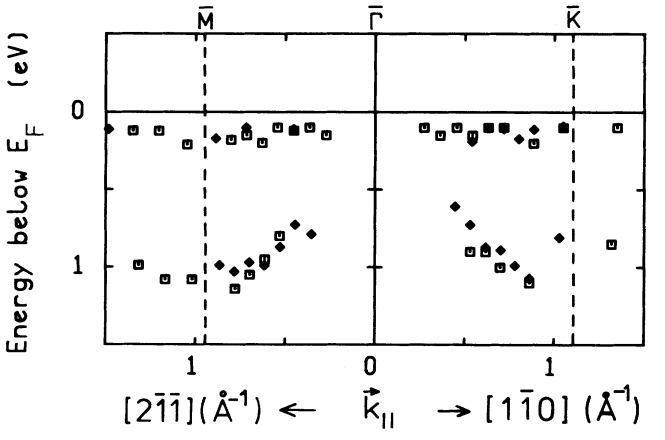

FIG. 10. Detailed surface-state dispersion along the $\bar{\Gamma}\bar{K}$ nd $\bar{\Gamma}\bar{M}$ directions of the Si(111)(7×7)-Pb surface. The experimental conditions and the symbols are similar to those in Fig. 9.

IV. ORIGIN OF THE SURFACE STATES AT THE Si(111)($\sqrt{3}\times\sqrt{3}$)R30°-Pb(β) SURFACE

Because Pb, Si, and Ge all belong to the group-IV elements, the heteropolar covalent binding between the Pb adatoms and the Si or Ge substrate is expected to be similar to the homopolar covalent binding of the Si or Ge adatoms at the clean reconstructed Si or Ge surfaces. For that reason, it is very useful to compare the Pb-induced surface states with the surface states at the clean reconstructed surfaces. This was done by Tonner *et al.* for the surface states at the Ge(111)($\sqrt{3}\times\sqrt{3}$)R30°-Pb(β) surface and the adatom induced states of the clean Ge(111)c(2×8) surface.[9] At the Ge(111)($\sqrt{3}\times\sqrt{3}$)R30°-Pb(β) surface, two surface states exist at 1.2 and 0.45 eV below the valence-band maximum. According to Tonner *et al.* these states are related to the S_3 and S_2 surface states of the clean reconstructed Ge(111)c(2×8) surface. The latter states are located at 1.35 and 0.65 eV below the VBM, respectively, and are interpreted as adatom and restatom states, respectively.[25] It is believed that these states are similar to the adatom and restatom states at the Si(111)(7×7) surface. The adatom state at the Si(111)(7×7) surface is at present well understood. It is composed of p_x and p_y orbitals of the adatom which are hybridized with Si dangling-bond states having wave vectors in the outer regions of the 1×1 SBZ or in the second $\sqrt{3}\times\sqrt{3}$ SBZ.[26] In much the same way, we will now compare the surface states at the Si(111)($\sqrt{3}\times\sqrt{3}$)R30°-Pb(β) surface with the surface states at the clean Si(111)(7×7) surface. We will discuss its energy position and dispersion.

In order to compare the surface-state energies of the Pb/Si(111) and Pb/Ge(111) surfaces with those of the clean reconstructed surfaces, the energies must be referred with respect to the VBM because different surfaces may have different pinning positions in the gap and a comparison of energies with respect to the Fermi level does not make sense. Because the pinning level of the Si(111)($\sqrt{3}\times3$)R30°-Pb(β) surface lies approximately 0.1 eV above the VBM, the energy of its lowest surface state is situated approximately 0.7 eV below the VBM. This should be compared to the energies of the surface state associated with the Pb adatoms on Ge(111) or Ge adatoms on Ge(111)c(2×8). These adatom states lie 1.2 and 1.4 eV below the VBM, respectively. So if the Ge adatoms on Ge(111) are replaced by Pb adatoms, the adatom surfaces states shift toward the VBM. This is consistent with the electronegativity difference between Pb and Ge. At the Si(111)($\sqrt{3}\times\sqrt{3}$)R30°-Pb(β) surface, the even larger electronegativity difference between Pb and Si also causes a larger upward shift of the Pb-induced surface state to 0.7 eV below the VBM of Si. The upward shift of these S_3 related surface states for the heavier adatoms is also apparent from a comparison with the ARUPS spectra of the Si(111)($\sqrt{3}\times\sqrt{3}$)R30°-Al, Si(111)($\sqrt{3}\times\sqrt{3}$)R30°-Ga, Si(111)($\sqrt{3}\times\sqrt{3}$)R30°-In, and Si(111)($\sqrt{3}\times\sqrt{3}$)R30°-Sn surfaces.[27,28] Also, the position of the S_3 related surface state at the Si(111)(7×7)-Ge and Si(111)(5×5)-Ge surfaces[29] is consistent with this view. Therefore, the energy of the lowest-lying surface state at the Si(111)($\sqrt{3}\times\sqrt{3}$)R30°-Pb(β) surface is fully compatible with the assignment of a Si dangling-bond state which is hybridized with Pb $6p_x,p_y$ orbitals.

Also the dispersion of this surface state seems to be in good agreement with this assignment. As shown in Figs. 9 and 10, this surface state appears in the outer parts of the 1×1 SBZ for both the Si(111)(7×7)-Pb and the Si(111)($\sqrt{3}\times\sqrt{3}$)R30°-Pb(β) surfaces. It disperses downward from 0.6 eV below E_F to approximately 1 eV below E_F at the zone boundary for both the $\bar{\Gamma}\bar{K}$ and $\bar{\Gamma}\bar{M}$ directions. This behavior is qualitatively similar to the surface-state dispersion at the Si(111)($\sqrt{3}\times\sqrt{3}$)R30°-In surface.[30] However, in our case a splitting of the surface-state bands at the $\bar{M}$ point is not observed. Also, it is not possible to estimate whether this surface has the symmetry of a $\sqrt{3}\times\sqrt{3}$ SBZ, because it cannot be observed in the first $\sqrt{3}\times\sqrt{3}$ SBZ. Nevertheless, based on the experimentally estimated dangling-bond character of this surface state and on its dispersion and energy, we attribute this surface state to a Si dangling-bond state, hybridized with Pb $6p_x,p_y$ orbitals.

The amount of Pb character of this surface state is not known. If this state is strongly localized on the Pb atoms, a much larger dispersion would be expected, because the Pb $6p_x,p_y$ orbitals must have a considerable overlap with the orbitals at neighboring Pb sites. The small dispersion (0.4 eV) indicates that there is only a limited degree of orbital overlap although the Pb layer is compressed having a mean in-plane interatomic distance of 3.4 Å. The temperature dependence of the surface state emission was investigated by Tonner *et al.*[31] for Pb on Ge(111) and by Le Lay and co-workers[6] for Pb on Si(111). The surface-state emission of Pb on Ge(111) shows a strong temperature dependence with a Debye temperature much lower than that of Ge but similar to that of Pb. This suggests that there must be a considerable contribution of Pb to the surface-state wave function. This behavior is not observed for Pb on Si(111) which led Le Lay and co-workers to the conclusion that the high-temperature 1×1 phase is not a liquid phase. However in our opinion, arguments based on this temperature dependence of the surface-state emission are not sufficient to make this assignment.

We will now turn to the discussion of the nature of the other surface state, i.e., the pinning state. This state is rather dispersionless and bears a strong resemblance to either the S_2 or S_1 surface states of the clean 7×7 structure which are dangling-bond-like. In order to understand the presence of the pinning state, we consider the bilayer model of Huang *et al.*[12] for the related Ge(111)($\sqrt{3}\times\sqrt{3}$)-Pb(β) surface. This structural model shows that there are four Pb atoms per $\sqrt{3}\times\sqrt{3}$ unit cell. One of the Pb atoms is chemisorbed at the H_3 site while three Pb atoms are placed on off-centered T_1 sites. The presence of two different types of Pb atoms per $\sqrt{3}\times\sqrt{3}$ unit cell made Huang *et al.* reach the conclusion that two different sets of surface states might be present. In the case that there is only one Pb atom per $\sqrt{3}\times\sqrt{3}$ unit cell occupying the H_3 site, we expect three states close to the valence-band edge with mainly dangling-bond character and three states close to the

conduction-band edge with mainly adatom character.[32] Two of the lowest-lying surface states are fully occupied and are lowered in energy by mixing with the p_x and p_y states of the adatom. The other low-lying dangling-bond state mixes with the adatom p_z state and is half filled. The presence of the off-centered T_1 atoms gives rise to another degenerate set of low- and high-lying surface states. The off-centered Pb atoms are less stabilized than the H_3 chemisorbed Pb atoms, so the surface states related to these off-centered atoms are closer to the Fermi level. Whereas this state is completely filled for the Pb/Ge system, it is partially filled for the Pb/Si system. In fact this might cause the strong pinning at the Pb/Si interface because the areal density of these states is about 10^{15} states/cm^2. There are no Fermi-level states at the Ge(111)($\sqrt{3}\times\sqrt{3}$)R30°-Pb(β) surface and to our knowledge, no band bending measurements of this surface have been reported.

The semiconducting nature of the Ge(111)($\sqrt{3}\times\sqrt{3}$)R30°-Pb(β) surface implies that there must be an even number of valence electrons per $\sqrt{3}\times\sqrt{3}$ unit cell in contrast to the Si(111)($\sqrt{3}\times\sqrt{3}$)R30°-Pb(β) surface which is metallic.[33] However, counting of the number of valence electrons present in the $\sqrt{3}\times\sqrt{3}$ cell always yields odd numbers (three Si or Ge dangling bonds plus four times the number of Pb adatoms). Even if the 6s states are fully occupied and situated far below the Fermi level, the total number of valence electrons will remain odd. Therefore, from a single-particle picture, one always expects a metallic surface, and so the semiconducting nature of the Pb/Ge(111) system is quite remarkable.

We note that the clean Ge(111)c(2×8) surface is semiconducting and remains semiconducting after deposition of Pb. The Si(111)(7×7) is metallic and remains metallic after deposition of Pb. The different electronic structures of the clean reconstructed surfaces are usually explained by differences between the 7×7 and the c(2×8) reconstructions. However, for the $\sqrt{3}\times\sqrt{3}$ surfaces, there are no differences between the two surface structures (and the number of valence electrons) so that an explanation based on differences in overlayer structures cannot hold. [The only difference between the two overlayers is the incommensurability of the Pb/Si(111) system, which probably has little influence on the local electronic structure].

From the data of Tonner *et al.*[9] it can be deduced that the uppermost surface state at the Ge(111)($\sqrt{3}\times\sqrt{3}$)R30°-Pb(β) surface is situated below the VBM throughout the whole Brillouin zone, whereas the corresponding state for the Pb/Si(111) system is situated 0.1 eV above the VBM. Therefore the surface states of the Pb/Ge(111) system must always be completely filled. If we really have an odd number of valence electrons per $\sqrt{3}\times\sqrt{3}$ unit cell, the large amount of charge needed for the complete filling of the surface-state bands of Pb on Ge(111) cannot be provided by donors alone, and the negatively charged surface must be compensated by valence-band holes. This might also explain the shift of the valence-band features of the Ge(111)($\sqrt{3}\times\sqrt{3}$)R30°-Pb(β) surface, found by Tonner *et al.*[9] They observed an upward shift of about 0.3 eV while the Fermi level of the Ge(111)c(2×8) surface is pinned only 0.1 eV above the VBM.[34,9] Therefore, if this shift is due to band bending, the Fermi level is situated below the VBM. Of course, this means that this surface must be metallic. However, the Fermi level must be close to the VBM, so it might be difficult to observe a Fermi edge with photoemission. A detailed core-level study on the Pb/Ge(111) system might shed some light on this hypothesis.

V. SURFACE STATES AND SCHOTTKY-BARRIER HEIGHT

We now come to a discussion of the main issue of this paper: the relationship between the electronic structure of the Pb/Si(111) surfaces and the SBH's of thick diodes, based on the same epitaxial interfaces. Generally, the agreement between SBH's inferred from C-V and I-V measurements and from photoelectron spectroscopy is poor.[35,7] Indeed, the SBH's of diodes having a Si(111)(7×7) interface differ significantly from the barrier heights established at monolayer coverage (0.70 and 0.94 eV, respectively.) On the other hand, the barrier heights for the $\sqrt{3}\times\sqrt{3}$ surfaces and the diodes having a $\sqrt{3}\times\sqrt{3}$ interface are much closer (0.93 and 1.04 eV, respectively; Fig. 12), suggesting that in that case essentially the same electronic state might be responsible for the pinning of the Fermi level. We argued that the surface state at E_F pins the Fermi level at a coverage of one monolayer. This pinning state probably transforms into a real interface state at a fully established interface. Such a state has to be localized at the interface and should therefore be situated in both the Si band gap and in a gap in the Pb band structure. A super-position of the projected band structures of Si and Pb (Fig. 13) shows that there is indeed a common gap near the Fermi level. It is situated around the M point of the 1×1 SBZ. The measured dispersion for the Pb-induced surface states is also drawn into the same figure. The pinning level is evidently present in this forbidden region. If this surface state survives after a thick layer has been deposited it will become a real interface state.

This argument applies to both types of interfaces. However, at the 7×7 interface, the pinning level returns

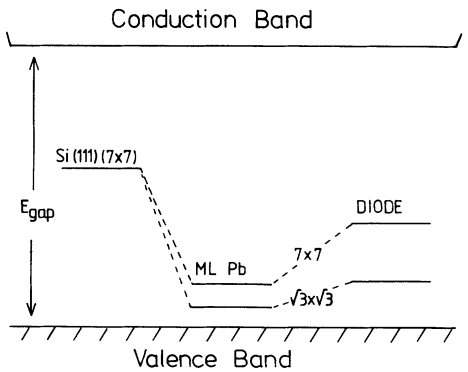

FIG. 12. Overview of measured Schottky-barrier heights.

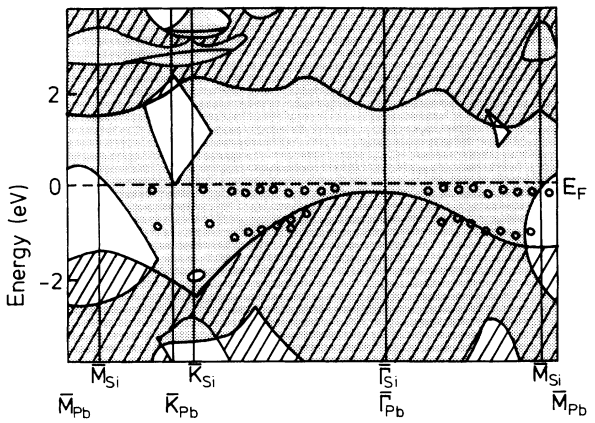

FIG. 13. Diagram showing the relation between the experimental surface-state dispersion of the Si(111)(7×7)-Pb surface (Fig. 10) and the bulk band structure of Si (hatched) and Pb (grey) along the $\bar{\Gamma}\bar{M}$ and $\bar{\Gamma}\bar{K}$ directions. Note that the Brillouin zone of Pb is slightly larger. The projected band structure of Pb is calculated with the localized spherical wave method (Ref. 38). Spin-orbit coupling is not included. The projected band structure of Si is taken from Ref. 39. The Pb-induced surface states are mainly present in the gap region of Si. The upper surface state is even crossing a region where Pb and Si have a common gap (close to the $\bar{M}$ points), suggesting that the Pb-induced surface state may survive below a thick layer of Pb as a real interface state.

to approximately the midgap position after depositing a thick Pb film. Its pinning might be due to metal-induced gap states, because the pinning position is close to the charge neutrality level.

The different behavior of the 7×7 and $\sqrt{3}\times\sqrt{3}$ interface cannot be explained by bulk properties, but must be related to the different interface structures. To what extent the original surface structures will remain intact is not certain for the $\sqrt{3}\times\sqrt{3}$ interface, but preliminary results with grazing-incidence x-ray diffraction show that the 7×7 symmetry of the Pb/Si(111) interface is preserved.[36] From this we may at least draw the conclusion that the interfaces below thick layers of Pb must be different because it is very unlikely that the $\sqrt{3}\times\sqrt{3}$ structure would return to a 7×7 structure. Additional evidence for this conclusion may be deduced from the fact that in both cases slightly rotated metastable domains are observed, but with distinctly different rotation angles.[36,8] In any case, it is likely that the orientation of the Pb overlayers will play an important role in determining the final position of the Fermi level. Because of the lack of registry for the Pb islands on top of the incommensurate $\sqrt{3}\times\sqrt{3}$ surface, a dangling-bond-like interface state might persist even at higher coverages. On the other hand, the islands are in parallel orientation with the intermediate 7×7-Pb layer, making mixing of surface states with bulk states of Pb more likely.

Finally, it should be pointed out that defect levels might be involved. However, the high number density of defect levels needed for pinnning is hardly compatible with the (well-characterized) ordered overlayer structures used in this study. The same conclusion was drawn in a recent study of the epitaxial $NiSi_2$/Si system by Vrijmoeth *et al.*[37]

VI. SUMMARY AND CONCLUSION

From the rigid shift of our UPS spectra, we determined the SBH's for two different epitaxial Pb layers on Si(111). The *n*-type SBH's of the Si(111)(7×7)-Pb and the Si(111)$(\sqrt{3}\times\sqrt{3})R30°$-Pb($\beta$) surfaces are 0.94±0.10 and 1.04±0.10 eV, respectively. Consequently, the Fermi-level position is very close to the valence-band edge. Two surface states were observed for both types of surfaces. One of them is situated approximately 0.9 eV below E_F while the other surface state crosses the Fermi level. The former state was interpreted as a Si dangling-bond state, which is hybridized with Pb $6p_x,p_y$ states. The latter state pins the Fermi level near the bottom of the energy gap, leading to the high Schottky barrier of diodes with the Si(111)$(\sqrt{3}\times\sqrt{3})R30°$-Pb($\beta$) interface. A similar state was reported for the Ge(111)$(\sqrt{3}\times\sqrt{3})R30°$-Pb($\beta$) surface but there it is situated entirely below the VBM so that this state is completely filled. For the Pb/Si(111) system, we argue that this state may become a genuine interface state at a fully established interface.

Many questions remain. The evolution of the surface states beyond a few-monolayers is not clear, in particular for the Si(111)(7×7)-Pb interface. Also the assignments proposed in this paper need confirmation. Inverse-photoemission spectroscopy and scanning tunneling miscroscopy may provide important complementary data about the nature and location of the pinning state. In addition, a slab-type calculation of a (commensurate) Si(111)$(\sqrt{3}\times\sqrt{3})R30°$-Pb($\beta$) interface seems feasible. This might prove the existence of true interface states. For such calculations, a precise knowledge of the structure of the deeply buried interface is required. Grazing incidence x-ray diffraction is a suitable tool for this purpose.

ACKNOWLEDGMENTS

We are grateful to Dr. T. S. Turner for her assistance with the photoemission experiments at the SERC Daresbury Laboratory. We would like to thank Professor C. Haas for his critical comments and A. Heeres for his technical assistance.

*Present address: Department of Physics, University of Pennsylvania, Philadelphia, PA 19104.

[1]D. R. Heslinga, H. H. Weitering, D. P. van der Werf, T. M. Klapwijk, and T. Hibma, Phys. Rev. Lett. **64**, 1589 (1990).

[2]R. T. Tung, Phys. Rev. Lett. **52**, 461 (1984); R. T. Tung, A. F. J. Levi, J. P. Sullivan, and F. Schrey, *ibid.* **66**, 72 (1991).

[3]J. Tersoff, Phys. Rev. Lett. **52**, 465 (1984).

[4]T. Hibma, H. H. Weitering, D. R. Heslinga, and T. M. Klapwijk, Appl. Surf. Sci. **48/49**, 209 (1991); H. H. Weitering, T. Hibma, D. R. Heslinga, and T. M. Klapwijk, Surf. Sci. **251/252**, 616 (1991).

[5]Whether or not there are states at the Fermi level, we will use the concept of Fermi-level pinning when the dipole charge is accomodated by interface states below E_F, because in that case, the Fermi-level position will be rather insensitive to the metal work function and the Mott-Schottky rule does not apply.

[6]G. Le Lay, K. Hricovini, and J. E. Bonnet, Appl. Surf. Sci. **41/42**, 25 (1989); G. Le Lay, M. Abraham, A. Kahn, K. Hricovini, and J. E. Bonnet, Phys. Scr. **T35**, 261 (1991).

[7]G. Le Lay and K. Hricovini, Phys. Rev. Lett. **65**, 807 (1990); H. H. Weitering, D. R. Heslinga, T. Hibma, and T. M. Klapwijk, *ibid.* **65**, 808 (1990).

[8]H. H. Weitering, D. R. Heslinga, and T. Hibma, Phys. Rev. B **45**, 5991 (1992).

[9]B. P. Tonner, H. Li, M. J. Robrecht, M. Onellion, and J. L. Erskine, Phys. Rev. B **36**, 989 (1987).

[10]R. Feidenhans'l, J. S. Pedersen, M. Nielsen, F. Grey, and R. L. Johnson, Surf. Sci. **178**, 927 (1986).

[11]B. N. Dev, F. Grey, R. L. Johnson, and G. Materlik, Europhys. Lett. **6**, 311 (1988).

[12]H. Huang, C. M. Wei, H. Li, B. P. Tonner, and S. Y. Tong, Phys. Rev. Lett. **62**, 559 (1989).

[13]G. Quentel, M. Gauch, and A. Degiovanni, Surf. Sci. **193**, 212 (1988).

[14]E. W. Plummer and W. Eberhardt, Adv. Chem. Phys. **49**, 533 (1982).

[15]G. V. Hansson and R. I. G. Uhrberg, Surf. Sci. Rep. **9**, 197 (1988).

[16]K. Hricovini and G. Le Lay (unpublished).

[17]F. J. Himpsel, G. Hollinger, and R. A. Pollack, Phys. Rev. B **28**, 7014 (1983).

[18]M. Alonso, R. Cimino, and K. Horn, Phys. Rev. Lett. **64**, 1947 (1990); A. Bauer, M. Prietsch, S. Molodtsov, C. Laubschat, and G. Kaindl, Phys. Rev. B **44**, 4002 (1991).

[19]S. Kono, K. Higashiyama, T. Kinoshita, T. Miyahara, H. Kato, H. Oshawa, Y. Enta, F. Maeda, and Y. Yaegashi, Phys. Rev. Lett. **58**, 1555 (1987).

[20]H. H. Weitering, Ph.D. thesis 1990, University of Groningen, 1990 (unpublished).

[21]G. Margaritondo, J. E. Rowe, and S. B. Christman, Phys. Rev. B **14**, 5396 (1976).

[22]V. Heine, Phys Rev. **138**, A1689 (1965).

[23]R. I. G. Uhrberg, G. V. Hansson, U. O. Karlsson, J. M. Nicholls, P. E. S. Person, S. A. Flodström, R. Engelhardt, and E. E. Koch, Phys. Rev. B **31**, 3795 (1985).

[24]According to A. Zur, T. C. McGill and D. L. Smith [Phys. Rev. B **28**, 2060 (1983)], only $10^{11}-10^{12}$ surface states/cm^2 are needed to pin the Fermi level at the surface. This amount is below the detection limit in UPS. Therefore, all Fermi-level states which show up in the UPS spectrum must have sufficient areal density to pin the Fermi level.

[25]J. Aarts, A. J. Hoeven, and P. K. Larsen, Phys. Rev. B **38**, 3925 (1988).

[26]J. E. Northrup, Phys. Rev. Lett. **57**, 154 (1986); **53**, 683 (1984).

[27]T. Kinoshita, S. Kono, and T. Sagawa, Phys. Rev. B **34**, 3011 (1986).

[28]T. Kinoshita, H. Ohta, Y. Enta, Y. Yaegashi, S. Suzuki, and S. Kono, J. Phys. Soc. Jpn. **56**, 4015 (1987).

[29]P. Mårtensson, W.-X. Ni, G. V. Hansson, J. M. Nicholls, and B. Reihl, Phys. Rev. B **36**, 5974 (1987).

[30]J. M. Nicholls, P. Mårtensson, G. V. Hansson, and J. E. Northrup, Phys. Rev. B **32**, 1333 (1985).

[31]B. P. Tonner, H. Li, M. J. Robrecht, Y. C. Chou, M. Onellion, and J. L. Erskine, Phys. Rev. B **34**, 4386 (1986).

[32]H. Nagayoshi, J. Phys. Soc. Jpn. **57**, 2105 (1988).

[33]An even number of valence electrons does not necessarily imply that the surface is semiconducting. Because many neighboring surface-state bands are involved, overlapping surface-state bands may render the surface metallic.

[34]W. D. Grobman, D. E. Eastman, and J. L. Freeouf, Phys. Rev. B **12**, 4405 (1975).

[35]F. Schäfler and G. Abstreiter, J. Vac. Sci. Technol. B **3**, 1184 (1985).

[36]F. Grey, M. Nielsen, R. Feidenhans'l, J. Bohr, J. S. Pedersen, J. B. Sørensen, R. L. Johnson, H. H. Weitering, and T. Hibma (unpublished); Weitering, Heslinga, and Hibma, Ref. 8.

[37]J. Vrijmoeth, J. F. van der Veen, D. R. Heslinga, and T. M. Klapwijk, Phys. Rev. B **42**, 9598 (1990).

[38]A. Kootte (unpublished).

[39]I. Ivanov, A. Mazur, and J. Pollman, Surf. Sci. **92**, 365 (1980).

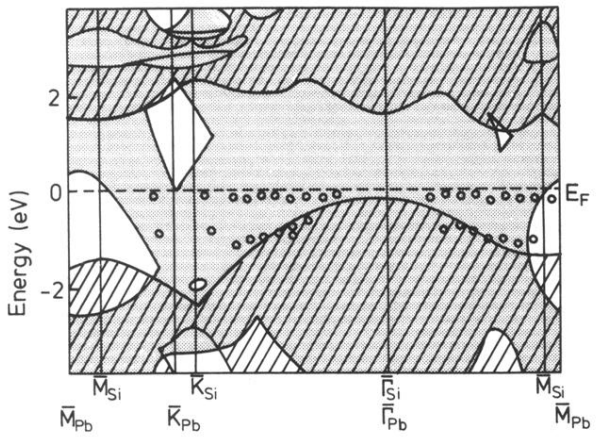

FIG. 13. Diagram showing the relation between the experimental surface-state dispersion of the Si(111)(7×7)-Pb surface (Fig. 10) and the bulk band structure of Si (hatched) and Pb (grey) along the $\bar{\Gamma}\bar{M}$ and $\bar{\Gamma}\bar{K}$ directions. Note that the Brillouin zone of Pb is slightly larger. The projected band structure of Pb is calculated with the localized spherical wave method (Ref. 38). Spin-orbit coupling is not included. The projected band structure of Si is taken from Ref. 39. The Pb-induced surface states are mainly present in the gap region of Si. The upper surface state is even crossing a region where Pb and Si have a common gap (close to the $\bar{M}$ points), suggesting that the Pb-induced surface state may survive below a thick layer of Pb as a real interface state.